IOP Conf. Series: Materials Science and Engineering **724** (2020) 012038 doi:10.1088/1757-899X/724/1/012038

The Effect of Working Parameters upon Oil-Lubricated EHD Contacts Subjected to Load Variation

X Zhang, R Glovnea

Department of Engineering and Design, University of Sussex, Brighton, BN1 9QT United Kingdom

E-mail: Xingnan.Zhang@sussex.ac.uk, R.P.Glovnea@sussex.ac.uk

Abstract. The technique of optical interferometry incorporated within a ball-on-disc apparatus has been widely used in the field of the experimental research in thin-film lubrication for approximately the past five decades. This paper presents the theoretical analysis of the dynamic response of an optical interferometry based experimental rig adapted for non-steady work. The dynamic response of the rig was analytically modelled as a three-degree of freedom, forced harmonic vibrating system with damping. Quantitative evaluation of damping of EHD contact was not one of the objectives of this paper, but the results obtained showed the opportunity to try a rather qualitative analysis. The aims of this experimental study are to investigate the effect of entrainment speed and overall film thickness on the oil film thickness of an EHD contact subjected to load cyclic variation. Experimental tests were carried out using different type of base oils with various viscosity. The behaviour of the EHD films was studied and analysed under forced harmonic load vibrations with frequency up to 100 Hz. The tests performed with lubricants of lower viscosity have shown that deviations from steady state film thickness become less and less pronounced as the viscosity of the lubricant decreases. When the amplitude of the oscillatory motion is significantly larger than the deformations of the surfaces under loading, it was observed that fluid entrainment is less important and film squeeze plays the dominant role in the film behaviour.

1. Introduction

Rolling bearings are the second most widely used machine components [1]. They work in what it is called elastohydrodynamic (EHD) lubrication regime. This lubrication regime is governed by the hydrodynamic action of the lubricant forced into a converging contact region, local surface deformations of similar magnitude to the lubricant film thickness and the variation of lubricant's viscosity with pressure. Under realistic working conditions, EHD contacts in rolling bearings are almost un-avoidably subjected to transient conditions such as variation of load and speed, passage of impurities, or vibrations generated by the equipment or machine they are part of. Transient conditions make the experimental measurement of EHD film thickness challenging. The influence of transient conditions of speed or load upon the behaviour of the elastohydrodynamic contacts has been investigated in the past, both experimentally and theoretically [2 – 5], however experimental studies dedicated to the effect of various working parameters on the formation of the EHD film, under load variation, are few. Glovnea and Spikes [6] and Wijnant et al [7] have shown that rapid change of speed, respective load induce fluctuations in the EHD film thickness. The amplitude of these fluctuations

decreases with time, after a few cycles, very much alike the dynamic response of a mass/spring/damper system. Kilali et al [8] reported a new test rig capable of loading an EHD contact both as an impact load and as a continuously variable load. The reported results were rather limited. Ciulli and Bassani [9] also used optical interferometry to study the film thickness in a contact subjected to random vibrations. Cann and Lubricht [10] studied the effect of low – frequency loading/unloading upon the track replenishment of a rolling EHD contact. They noticed the beneficial effect of these conditions upon the lubricant film thickness.

The behaviour of EHD films subjected to vibrations normal to the plane of the contact is influenced by two mechanisms: fluid entrainment and film squeeze. These mechanisms shape two phenomena which determine the lubricant film thickness: the dynamic response of the film and its deviation from normal EHD film shape.

This paper firstly presents the analysis of dynamic response of an optical interferometry based experimental rig adapted for non-steady work in the experimental setup section. Quantitative evaluation of the damping of EHD contacts was not one of the initial objectives of this research, but the results obtained showed the opportunity to try a rather qualitative analysis. Secondly, experimental results of the effect of entrainment speed and overall film thickness on the oil film thickness in an EHD contact subjected to load variation are shown and discussed.

2. Experimental rig setup and dynamic response analysis

The experimental method for measuring film thickness in this paper is the optical interferometry technique. The principle of optical interferometry and its various ways in which it is applied to the study of elastohydrodynamic contacts has been published extensively during the past fifty years [11-15] and it will not be detailed in this paper.

Figure 1a shows a sketch of the test rig while Figure 1b shows the schematic of the vibrating masses.

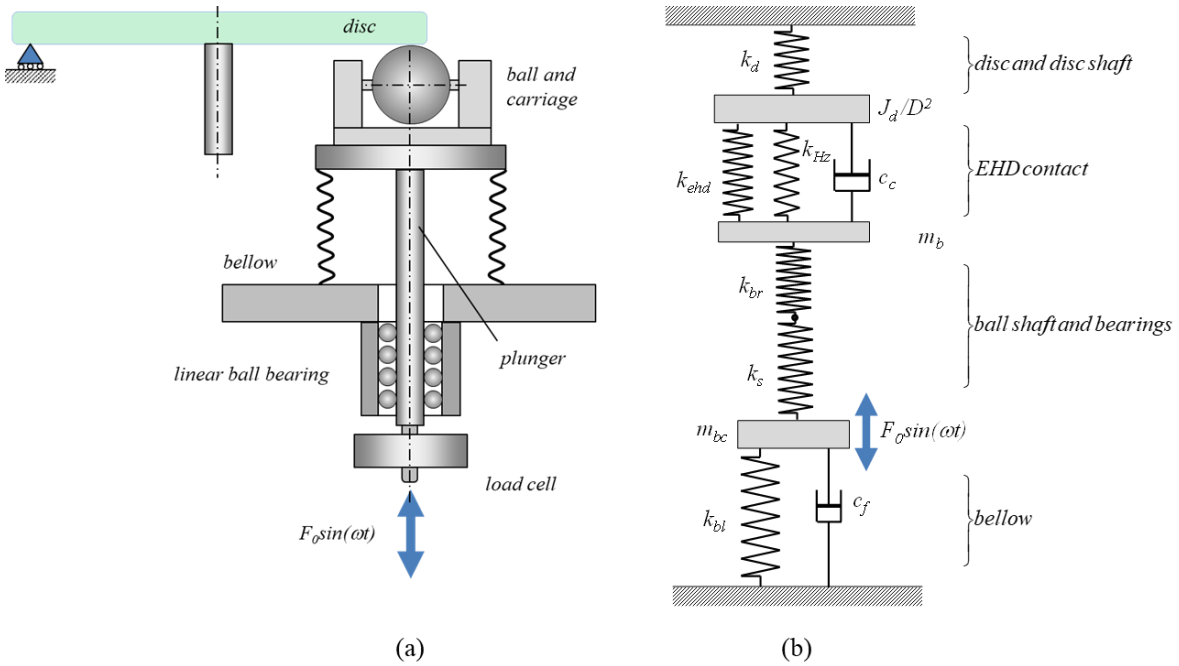

(a) (b)

Figure 1. (a) Schematic of experimental rig (b) Model of the vibrating system

Details of film thickness calibration procedure and experimental hardware introduction are provided in [17]. In order to increase the stiffness of the disc and its shaft, the disc is supported at a location diametrically opposite the ball, by a rolling support shown schematically like a simple support

in figure 1. The load cell records the variable force applied to the plunger and thus to the ball and the EHD contact. The stainless-steel bellow is intended to avoid any leakage of lubricant from the working chamber, but its construction makes it practically a linear spring. As seen in figure 1b the EHD contact acts as a spring and damper; its stiffness and damping coefficient are denoted with k_c and c_c respectively. The contact (as an elastic element of stiffness k_{Hz}) is connected to the oscillating mass of the ball m_b via the shaft supporting the ball and the bearings supporting the ball shaft. The stiffness of these elements is denoted by k_s for the shaft and k_{br} for the bearings. The contact "spring" is connected to the fixed support through the disc which is considered a spring of constant k_d. The second mass of this system is that of the ball carriage and plunger denoted by m_{bc}. These at their turn are connected to the rigid support through the bellow seen as a spring of stiffness k_b. There is also friction in the linear bearing supporting the plunger, represented here by the damping c_f. This is a three-degree of freedom, forced vibration system with damping, which can be solved for the motion of the mass of the ball and disc, which are of interest.

The stiffness of the dry Hertzian contact can be found from the relationship between the displacement of two distant points and the load, as shown below.

$$\delta = \left(\frac{9P^2}{16E^{*2}R} \right)^{1/3} \tag{1}$$

Obviously the EHD contact is a non-linear spring with the stiffness depending on the load. The stiffness of the dry Hertzian contact is obtained by inversing the ratio of the derivative of the displacement with respect to the load P, as shown below.

$$k_{Hz} = \frac{dP}{d\delta} = \left(6E^{*2}RP\right)^{1/3} \tag{2}$$

This stiffness varies with load can be seen in figure 2. After a sharp rise at lower loads the gradient of the curve becomes smaller and the curve would eventually flatten out at much higher loads.

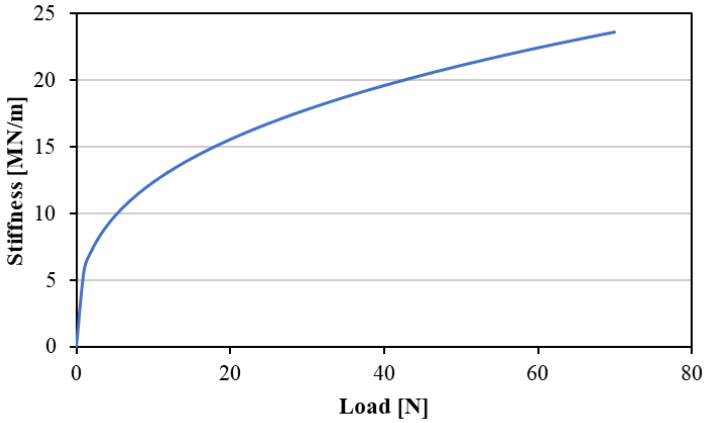

Figure 2. Stiffness of contact variation with load

This small change of the stiffness with load, at loads higher than about 4 N, prompts an approximation: the dry Hertzian contact can be considered as a linear spring, over the most part of the loading cycle.

The EHD film also depends on the load, so it too can be considered as a non-linear spring. In order to find the stiffness of this spring, the same method is applied. The central film thickness for a circular contact is given by the relationship:

$$\frac{h_c}{R_x}=2.69\overline{U}^{0.67}\overline{G}^{0.53}\overline{P}^{-0.067} \tag{3}$$

Where $\bar{P}$ is the load factor, $\bar{G}$ is the material parameter and $\bar{U}$ is speed parameter. Grouping all factors that do not depend on the load in one constant A, and differentiating film thickness with respect to the load, the inverse ratio yields the stiffness of the EHD film:

$$k_{EHD}=\frac{\partial P}{\partial h}=-\frac{15}{A}\cdot P^{32/30} \tag{4}$$

The variation of this stiffness with the load is depicted in figure 3.

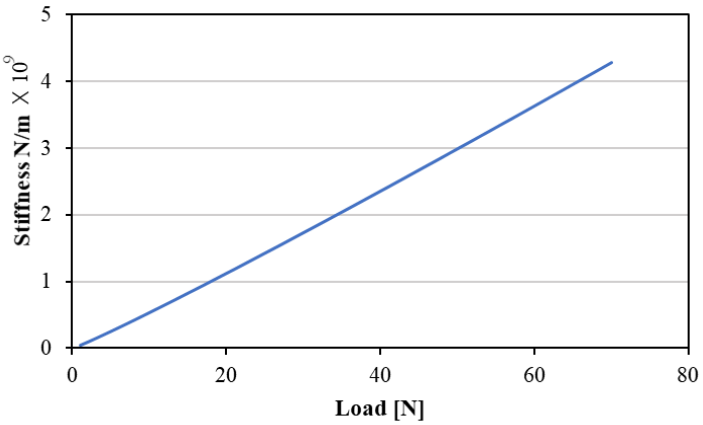

Figure 3. Stiffness of the EHD film.

The stiffness of the dry contact and that of the EHD film are connected in series thus the combined stiffness is given by:

$$\frac{1}{k_c}=\frac{1}{k_{Hz}}+\frac{1}{k_{EHD}} \tag{5}$$

By comparing the values of stiffness in figure 2 and 3, it is seen that the stiffness of the EHD film is two orders of magnitude larger than that of the dry Hertzian contact, thus from equation above it is clear that the later dominates the stiffness of the whole EHD contact. It thus appears that the stiffness of the EHD contact is equal to that of the dry Hertzian contact and it can be assumed a linear spring, according to the approximation mentioned above, which simplifies considerably the modelling of the whole system.

On the other hand, the damping constant of the EHD film (c_c) can also be assumed as non – linear and it is unknown at this stage. For the sake of simplicity of this analysis, it is further assumed that the damping is of viscous type, thus the motion – resisting force is proportional to the speed. Detailed stiffness calculations and comparisons of experimental parts showed in figure 1(b) as well as EHD friction force results are presented in [16]. With the mechanical characteristics of the system known, the equations of motion can be written as:

$$\begin{bmatrix} 1 & 0 & 0 & 0 & 0 & 0 \\ 0 & 1 & 0 & 0 & 0 & 0 \\ 0 & 0 & 1 & 0 & 0 & 0 \\ 0 & 0 & 0 & m_{bc} & 0 & 0 \\ 0 & 0 & 0 & 0 & m_b & 0 \\ 0 & 0 & 0 & 0 & 0 & J/D^2 \end{bmatrix} \frac{d}{dt} \begin{bmatrix} x_{bc} \\ x_b \\ x_d \\ \dot{x}_{bc} \\ \dot{x}_b \\ \dot{x}_d \end{bmatrix} + \begin{bmatrix} 0 & 0 & 0 & -1 & 0 & 0 \\ 0 & 0 & 0 & 0 & -1 & 0 \\ 0 & 0 & 0 & 0 & 0 & -1 \\ (k_{bl}+k_b) & -k_b & 0 & 0 & 0 & 0 \\ -k_b & (k_b+k_c) & -k_c & 0 & c_c & -c_c \\ 0 & -k_c & (k_c+k_d) & 0 & -c_c & c_c \end{bmatrix} \begin{bmatrix} x_{bc} \\ x_b \\ x_d \\ \dot{x}_{bc} \\ \dot{x}_b \\ \dot{x}_d \end{bmatrix} = \begin{bmatrix} 0 \\ 0 \\ 0 \\ 0 \\ F_0 \\ 0 \end{bmatrix} \cos \omega t \tag{6}$$

In this equation $\dot{x}_b$, $\dot{x}_{bc}$ and $\dot{x}_d$ are the velocities of the ball, ball carriage and disc respectively, while J is the moment of inertia of the disc about an axis (perpendicular to the plane of the drawing) passing through the fixed support shown in figure 1.

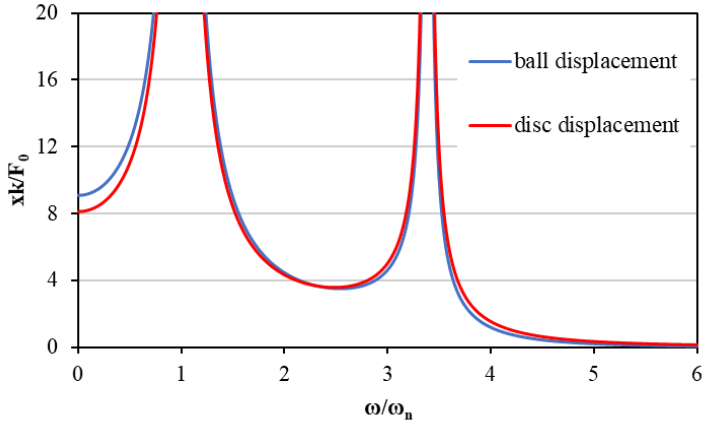

Figure 4. Displacement of ball and disc

The normalised displacements of the ball and the disc which are of interest here are shown in figure 4. Stiffness k and amplitude of the load F0, in these graphs were taken as 14,314MN/m and 20 N respectively. The first mode for the oscillations of the ball and disc is at 2140 Hz and the second is at 7270 Hz. Obviously, these are much larger than the frequency of variation of the force employed in these tests. The absolute values of the displacement of the ball and disc are of no real practical interest, but the difference between them it is. The variation of this difference is shown in figure 5, for frequencies around the first mode, which are more relevant in any applications.

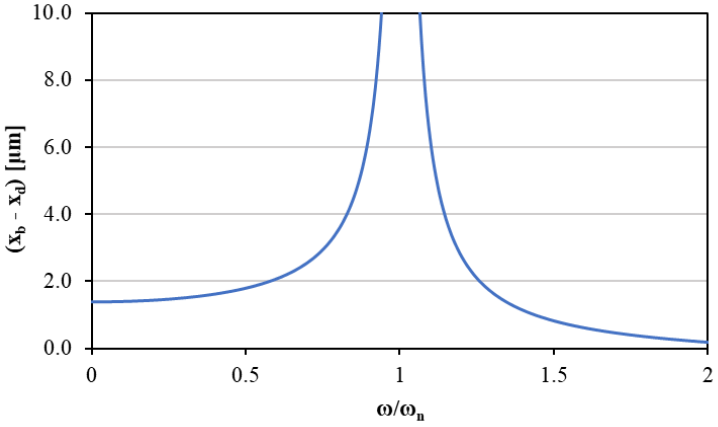

Figure 5. Displacement of the ball relative to the disc

The displacement of the ball relative to the disc is shown in real values instead of normalised ones. This gives a better idea of how realistic this simulation is. It can be seen that the value, 1.39 μm, at the largest frequency of the test that is 100 Hz ($\omega/\omega_n = 0.046$), is remarkably close to the amplitude resulted from Hertz's theory, which is 1.67 μm. The damping constant used in the above calculations varied between 0.01 Ns/m and 314 Ns/m, but the results show that at least at lower frequencies the displacement of the masses is insensitive to this parameter. There are other observations which can be withdrawn from this analysis. If the disc is made rigid, then the natural frequencies of the system shift toward larger values. For example, the first mode changes from 2140 Hz to 3600 Hz. The degree of freedom of the system reduces by one in this case. For a two–degree of freedom the system's response changes with the damping constant, but only at larger frequencies. This is shown in figure 6, where the response of a two–degree of freedom system is shown. As seen, the values of the damping constant change the response visibly, only at frequencies around the second mode.

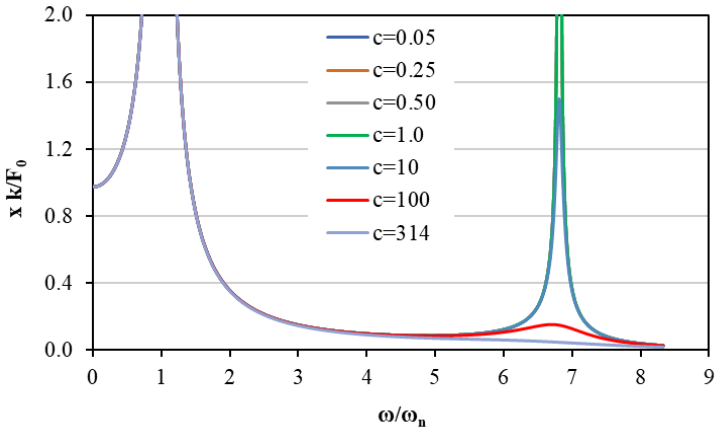

Figure 6. Response of the system

This theoretical dynamic analysis can be used to evaluate the damping constant of the EHD films. By attaching a large mass to the ball carriage, the natural frequency of the system can be lowered to values around 70 Hz – 80 Hz, which is within the range conveniently covered by the current optical system. Subsequently measuring the lubricant film thickness over a sweep of frequencies, encompassing the natural system, the damping characteristics of the EHD film can be evaluated by fitting the model to the experimental values. This is planned for future research.

3. Test condition and lubricants

The load was varied sinusoidally from zero (or close to zero) to about 40 N. For the pair of materials used which have a reduced elastic modulus E' =55GPa, this means a Hertzian pressure variation between zero and around 0.64 GPa. The frequency of the oscillatory motion of the ball (19.05 mm diameter) was 100 Hz throughout these tests. In order to get a good number of images for each cycle of oscillation, even at larger frequencies, a speed of 2000 frames per second was set on the camera. Many lubricants were tested in this research, but for limitations of space only the results for lubricants of three different viscosities will be shown. The kinematic viscosities at are: *Lubricant 1* - 339.8 mm^2/s, *Lubricant 2* - 135.8 mm^2/s and *Lubricant 3* - 17 mm^2/s.

4. Result and discussion

Experimental tests regarding the effect of overall film thickness of EHD contact subjected to load variation were carried out with two types of lubricant at different experimental working conditions. The images shown in Figure 7 were recorded at 100 Hz with an entrainment speed of 0.05 m/s for *Lubricant 1*, images of figure 8 are for *Lubricant 2*, and images of figure 9 are for *Lubricant 3*. The

images shown in figure 13 were also recorded at 100 Hz with a slightly increased entrainment speed of 0.1 m/s for *Lubricant 3*. Loading conditions for figure 7, figure 8 and figure 9 were identical, however the load variation for figure 13 is between 0 N and 39 N.

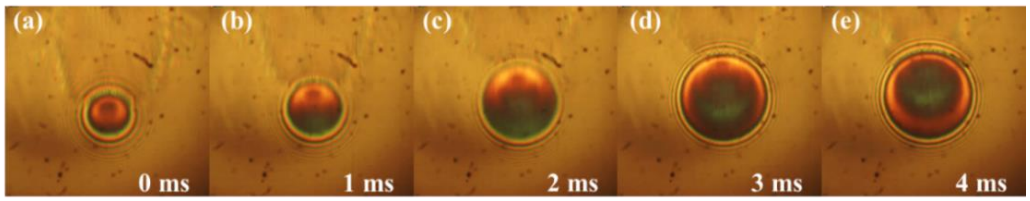

Figure 7. Selected images of the EHD contact for 100 Hz, 0.05 m/s, Lubricant 1.

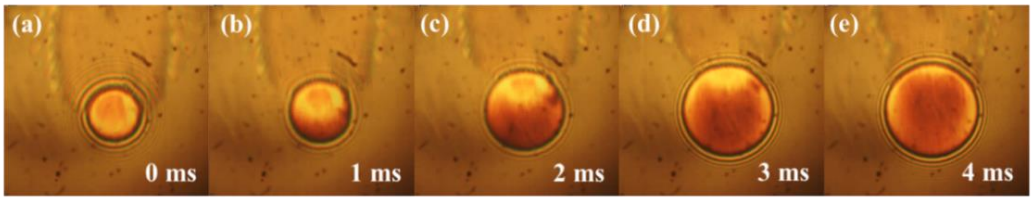

Figure 8. Selected images of the EHD contact for 100 Hz, 0.05 m/s, Lubricant 2.

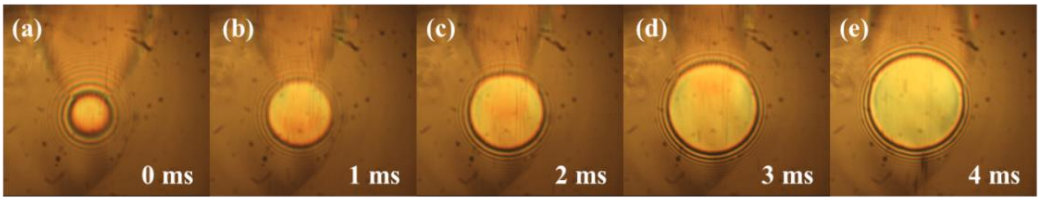

Figure 9. Selected images of the EHD contact for 100 Hz, 0.05 m/s, Lubricant 3.

It has shown that the deviations from steady state film thickness become less and less pronounced as the viscosity of the lubricant decreases. This is illustrated by the captured images shown in figures 7-9. In terms of the actual values of the film perturbation, the difference is more obvious in figures 10 – 12, which captures the film thickness profile at the same time during the loading cycle for Lubricant 1-3 respectively. As seen, film perturbations of 62 nm for Lubricant 1, around 22 nm for Lubricant 2, and around 11 nm for Lubricant 3 are formed during the load variation cycle.

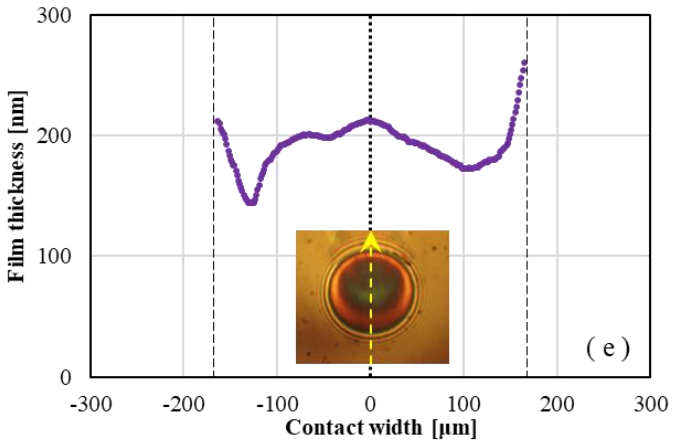

Figure 10. Film thickness profile, 100 Hz, *lubricant 1*.

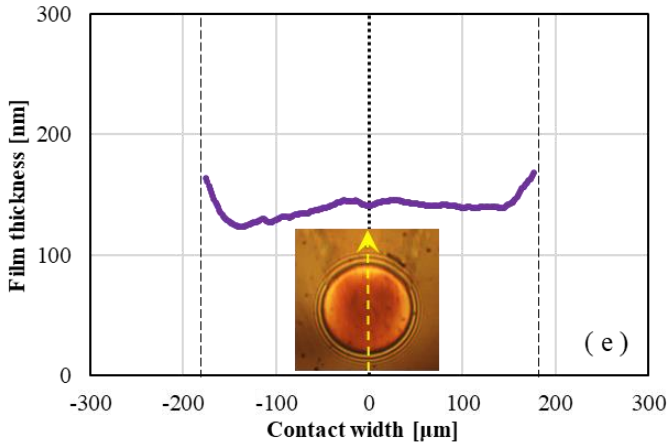

Figure 11. Film thickness profile, 100 Hz, *lubricant 2*.

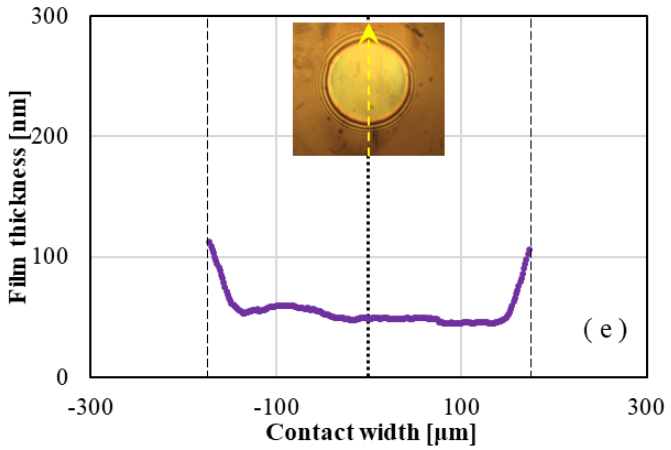

Figure 12. Film thickness profile, 100 Hz, *lubricant 3*.

From the above analysis it is clear that the lower the viscosity of the lubricant, thus the film thickness in steady-state conditions are, the smaller the film perturbation formed during transient loading conditions. This conclusion is apparently contradicted by the results shown in figures 13 and 14 which were taken for Lubricant 3 which has the smallest viscosity among the oils tested here. Even at an entrainment speed of 0.1 m/s this gives a central film thickness of about 50 nm in steady state conditions, lower than the other two lubricants. As seen in Figure 14 this lubricant forms an entrapment of 220 nm which obviously is larger than those formed by the other two lubricants.

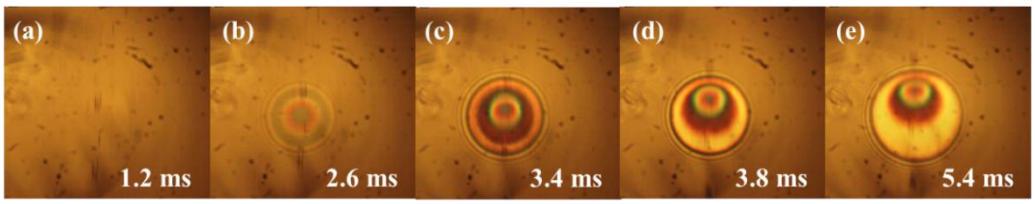

Figure 13. Selected images of the EHD contact for 100 Hz, 0.1 m/s, Lubricant 3.

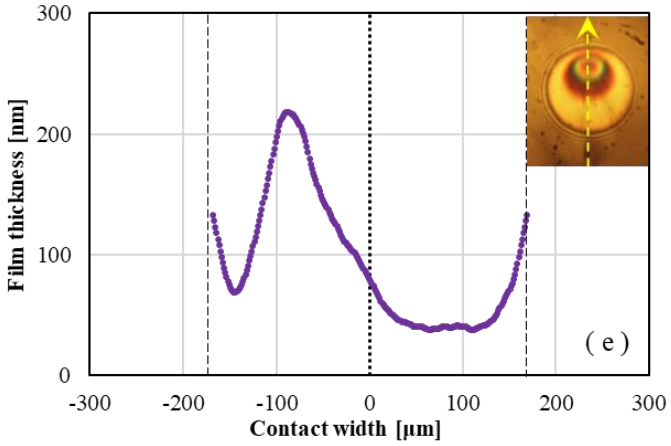

Figure 14. Film thickness profile, 100 Hz, 0.1 m/s, *lubricant 3*.

This phenomenon can only happen when the amplitude of the oscillatory motion is significantly larger than the deformations of the surfaces under loading. In this case the rebounding of the surfaces is large which in turn generate large impact forces. The fluid entrainment is less important in this situation and film squeeze plays the dominant role in the film behaviour. In a way, this is similar to pure squeeze or sudden halting of motion, where larger dimples are formed and trapped inside the contact. In this particular test the maximum height of the perturbation is nearly 4.5 times greater than the value under steady state condition. This implies that impact loading always generates perturbations to the film thickness no matter what the overall film thickness is.

5. Conclusions

This paper shows results of a larger study on the effect of cyclic load variation upon the film thickness of elastohydrodynamic contacts. It also includes a simplified analysis of the dynamic response of an optical interferometry based experimental rig. The dynamic response has been analytically modelled as a three-degree of freedom, forced harmonic vibrating system with damping. Results show that this dynamic analysis can be extended into evaluating the damping constant of EHD films by attaching a large mass to the ball carriage to lower the natural frequency of the whole system.

Experimental tests were carried out using a number of fluids with varied viscosity. The behaviour of the EHD films was studied and analyzed under forced harmonic load vibrations at a frequency of 100 Hz. The test performed with lubricants of lower viscosity have shown that deviations from steady state film thickness become less and less pronounced as the viscosity of the lubricant decreases. When the amplitude of the oscillatory motion is significantly larger than the deformations of the surfaces film perturbation still occurs because in this case film squeeze dominates the fluid entrainment as the mechanism which influences the film.

6. References

[1] Lugt, P. M., 2013, "*Grease Lubrication in Rolling Bearings*", John Wiley and Sons.
[2] Dowson, D., and Higginson, G. R., 1959, "A Numerical Solution to the Elastohydrodynamic Problem", *J. Mech. Eng. Sci.*, **1**, pp 6-15.
[3] Safa, M. M. A., and Gohar, R., 1986, "Pressure Distribution under a Ball Impacting a Thin Lubricant Layer", *Trans. ASME, J. Trib*, **108**, pp 372-376.
[4] Sugimura, J., Jones, W. R. Jr, and Spikes, H. A., 1998, "EHD Film Thickness in Non-Steady State Contacts", *Trans. ASME, J. Trib*, **120**, pp 442-452.
[5] Sakamoto, M., Nishikawa, H., and Kaneta, M., 2003, "Behavior of Point Contact EHL Films under Pulsating Loads", *Transient Processes in Tribology,* Elsevier, **43**, pp 391-399.
[6] Glovnea, R.P. and Spikes, H.A., 2001, "Elastohydrodynamic Film Collapse During Rapid Deceleration-Part I: Experimental Results", *Trans. ASME, J. Trib*, **123**, 2, pp 254-261.

[7] Wijnant, Y. H., Venner, C.H., Larsson, R. and Ericsson, P., 1999, "Effects of Structural Vibrations on the Film Thickness in an EHL Circular Contact", *J. Trib*, **121**, pp 259-264.
[8] Kilali, T. El., Perret-Liaudet, J. and Mazuyer, D., 2003, "Experimental Analysis of a High Pressure Lubricated Contact under Dynamic Normal Excitation Force", *Transient Processes in Tribology*, Elsevier, **43**, pp 409-417.
[9] Ciulli, E. and Bassani, R., 2006, "Influence of Vibrations and Noise on Experimental Results of Lubricated non-Conformal Contacts", *Proc. IMechE.*, **J220**, pp 319-331.
[10] Cann, P. M. and Lubrecht, A. A., 2003, "The Effect of Transient Loading on Contact Replenishment with Lubricating Greases", *Transient Processes in Tribology*, Elsevier, pp 745-750.
[11] Françon, M., 1966, "Optical Interferometry", *Academic Press*
[12] Cameron, A., and Gohar, R., 1966, "Theoretical and Experimental Studies of the Oil Film in Lubricated Point Contacts", *Proc. R. Soc. Lond. A*, **291**, pp 520-536.
[13] Gohar, R. and Cameron, A., 1967, "The Mapping of Elastohydrodynamic Contacts", *ASLE Trans*, **10**, pp 215-225.
[14] Foord, C. A., Hammann, W. C. and Cameron, A., 1968, "Evaluation of Lubricants Using Optical Elastohydrodynamics', *ASLE Trans*, **11**, pp 31-43.
[15] Wedeven, L. J, 1970, "Optical Measurements in Elastohydrodynamic Rolling Contact Bearings", PhD. thesis, London University, London.
[16] Zhang. X, 2017, "The Effect of Vibrations on the Behavior of Lubricated Elastohydrodynamic Contacts. PhD thesis, University of Sussex.
[17] Glovnea, R.P and X. Zhang, 2018, "Elastohydrodynamic Films under Periodic Load Variation: An Experimental and Theoretical Approach", *Trib. Lett*, **66**, pp116.